Accepted Manuscript

The novel anthracene decorated dendrimeric cyclophosphazenes for highly selective sensing of 2,4,6-trinitrotoluene (TNT)

Emrah Özcan, Süreyya Oğuz Tümay, Gürkan Keşan, Serkan Yeşilot, Bünyemin Çoşut

PII:	S1386-1425(19)30496-2
DOI:	https://doi.org/10.1016/j.saa.2019.05.020
Reference:	SAA 17115
To appear in:	*Spectrochimica Acta Part A: Molecular and Biomolecular Spectroscopy*
Received date:	31 December 2018
Revised date:	9 May 2019
Accepted date:	10 May 2019

Please cite this article as: E. Özcan, S.O. Tümay, G. Keşan, et al., The novel anthracene decorated dendrimeric cyclophosphazenes for highly selective sensing of 2,4,6-trinitrotoluene (TNT), Spectrochimica Acta Part A: Molecular and Biomolecular Spectroscopy, https://doi.org/10.1016/j.saa.2019.05.020

The Novel Anthracene Decorated Dendrimeric Cyclophosphazenes for Highly Selective Sensing of 2,4,6-Trinitrotoluene (TNT)

Emrah Özcan, Süreyya Oğuz Tümay, Gürkan Keşan, Serkan Yeşilot, Bünyemin Çoşut*

Department of Chemistry, Faculty of Science, Gebze Technical University, Gebze, Kocaeli, Turkey

*Corresponding author: Department of Chemistry, Faculty of Science, Gebze Technical University, Gebze, Kocaeli, Turkey, Phone: +902626053015, e-mail: bc@gtu.edu.tr

Abstract

Novel fluorescent anthracene-decorated cyclotri- and cyclotetraphosphazenes (**5** and **6**) are designed and synthesized, and their chemosensor behaviors against nitroaromatic compounds are examined by UV/Vis and fluorescence spectroscopies for addressing the sensors with cyclophosphazenes for 2,4,6-trinitrotoluene detection. The fluorescence intensities of (**5** and **6**) are found to be selectively quenched by only 2,4,6-trinitrotoluene through the non-covalent π···π stacking interactions between anthracene-substituted cyclophosphazenes and 2,4,6-trinitrotoluene. In addition, cyclic voltammetry and theoretical calculation of novel sensor systems are studied. The proposed fluorescent sensor systems are critical in terms of practical detection of 2,4,6-trinitrotoluene.

Keywords: Phosphazenes, Explosive, TNT, Fluorescence, Nitroaromatic, Chemosensor, Detection limit

1. Introduction

The sensing of nitroaromatic compounds (NACs) such as picric acid and 2,4,6-trinitrotoluene (TNT) by novel fluorescent chemosensors in order to increase the selectivity and sensitivity of previously reported systems have been one of the issues of the supramolecular chemistry [1]. TNT is one of the most widely used NACs and detection of TNT is critical in owing to concerns on environmental protection and global security [2]. Various analytical techniques such as chromatographic techniques [3], electrochemical detection [4], chemiluminescence detection [5], fluorescent monitoring [6], gas chromatography [7] and high-performance liquid chromatography [8] have been used for detection and determination of NACs. Although instrumental techniques are selective and sensitive, most of these devices are rather bulky, expensive, time consuming and requiring laboratory conditions with expert users. Thus, fluorescence-based sensing which is highly sensitive, convenient, and cost effective has been attracted academy and industry. Hence, a wide variety of fluorescent sensor such as organic/inorganic polymeric materials [9, 10], metal organic materials [11, 12], covalent organic polymers and dendrimers [13-15] and quantum dots [4, 16] have been prepared recently and screened for detection of NACs. In addition to these detection systems, π-electron-rich small molecules have become alternative fluorescent sensors for detection of NACs [17, 18].

Small molecules as a fluorescent sensor are attractive because of their high quantum yield, straightforward synthesis, better reproducibility and easy purification. Therefore, the design and preparation of the conformationally strict π-electron-rich systems have fascinated considerable attention in recent years due to their strong π···π piling interactions resulting in mainly fluorescent quenching process [19].

Cyclophosphazenes are important compounds for preparation of novel fluorescent systems as substituted groups on phosphorus atoms can be used as various terminal groups for fluorescence detection [20, 21]. In addition, optical properties of cyclophosphazene

derivatives could be tuned by substituents on phosphorus, as the cyclophosphazenes scaffold is optically inert in UV–Vis region which is playing an important role in the design of cyclophosphazene-based detection systems [22]. Commercially available hexachlorocyclotriphosphazene, $N_3P_3Cl_6$, and octachlorocyclotetraphosphazene, $N_4P_4Cl_8$, are fascinating compounds. They exhibit high thermal stability and are extremely sensible to nucleophilic reactions under basic conditions. Thus, those compounds allow the preparation of a variety of cyclophosphazene-based materials. Also, hexakis- and octakis-cyclophosphazenes display intramolecular excimer emission through the non-covalent π···π piling interactions between the anthracene moieties [23-28].

According to previous reports on detection of NACs, strong π···π stacking interactions between electron-rich cyclophosphazene-based systems and NACs led to non-selective detection of NACs [29]. In the present study, we provide strong π···π interactions between the TNT and anthracene through cyclophosphazene platform. We chose anthracene as a chromophore to provide strong π···π interactions. We synthesized hexakis(4-hydroxyphenylanthracene-9-carboxylate) cyclotriphophazene (compound **5**), octakis(4-hydroxyphenylanthracene-9-carboxylate) cyclotetraphophazene (compound **6**) (Figure 1) and characterized those compounds by standard spectroscopic techniques such as ^{1}H, ^{13}C and ^{31}P NMR, and mass spectrometry (MALDI-TOF). In addition, to understand the effect of cyclophosphazene core on sensor properties of compounds **5** and **6**, phenyl anthracene 9-carboxylate (precursor) was synthesis according to the literature [30] and its molecular structure was determined by X-ray crystallography. All the characterization data for synthesized compounds are given in Supporting information (Figure S1-S9). After synthesis and characterization, we tested the sensor properties of novel compounds to sense TNT and showed the important potential of the compounds on the sensing of TNT.

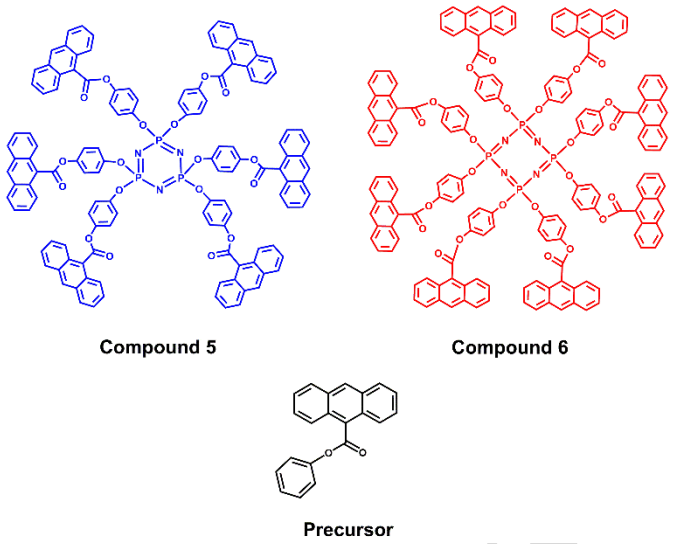

Figure 1. The molecular structures of compound **5**, compound **6** and the precursor.

2. Materials and Methods

All chemicals were reagent grade quality and obtained from commercial suppliers. While the deuterated solvents $CDCl_3$ and $(CD_3)_2CO$, cyclohexene, ethanol, 4-benzyloxyphenol, $Pd(OH)_2$, 4-Dimethylaminopyridine (DMAP), N,N'-Dicyclohexylcarbodiimide (DCC), Cs_2CO_3, acetonitrile, silica gel 60, 9-Anthracenecarboxylic acid and tetrahydrofuran was purchased from Merck, 1,8,9-Anthracenetriol (for MALDI analysis) was obtained from Fluka. Hexachlorocyclotriphosphazene (trimer) and octachlorocyclotetraphosphazene (tetramer; Otsuka Chemical Co. Ltd) were purged by using by fractional crystallization with n-hexane.

2.1. Equipments

Electronic absorption in the UV-visible region, fluorescence excitation and emission spectra were measured by Shimadzu 2101 and Varian Eclipse spectrofluorometer, respectively, using 1 cm pathlength cuvettes at room temperature. Horiba-Jobin-Yvon-SPEX Fluorolog 3-2iHR instrument with Fluoro Hub-B Single Photon Counting Controller were used to calculate fluorescence life time for excitation at 390 nm. Signal acquisition was carried out TCSPC module. Mass spectra were obtained by Bruker Daltonics Microflex mass spectrometer

(Bremen, Germany) equipped with a nitrogen UV-Laser operating at 337 nm in linear modes with average of 50 shots. ^{1}H, ^{13}C and ^{31}P NMR spectra were setted in $CDCl_3$ or deuterated acetone solutions down with a Varian 500 MHz spectrometer. Analytical thin layer chromatography (TLC) was implemented on silica gel plates (Merck, Kieselgel 60A, 0.25 mm thickness) with F_{254} indicator. Column chromatography was applied on silica gel (Merck, Kieselgel 60A, 230-400 mesh).

2.2. X-ray data collection and structure refinement

The X-Ray data were obtained with Bruker APEX II QUAZAR three-circle diffractometer. Indexing was performed by using APEX [31]. Data integration and reduction were achived with SAINT V8.34A [32]. Absorption correction was executed by multi-scan method implemented in SADABS V2014/5 [33]. The structures were elucidated and clarified by Bruker SHELXTL Software Package [34]. The final geometrical parameters and the molecular drawings were completed using with Platon (version 1.17) and Mercury CSD (version 3.5.1) programs [35, 36]. Structural determination has been stored to the Cambridge Crystallographic Data Centre with references CCDC 1541931 for structure precursor.

2.3. Synthesis

2.3.1. Synthesis of compounds 1-4 and precursor

The compounds **1-4** and precursor were synthesized and purified according to the literature procedure (Scheme S1 in SI) [25-27, 30, 37].

2.3.2. Synthesis of compound 5 (hexakis(4-hydroxyphenylanthracene-9-carboxylate) cyclotriphophazene)

A mixture of 2,2,4,4,6,6 hexakis-(hydroxyphenoxy) cyclotriphosphazatriene (**2**; 31 mg, 0.04 mmol), 9-Anthracenecarboxylic acid (71 mg, 0.32 mmol), DMAP (129 mg, 1.064 mmol) and DCC (156 mg, 0.76 mmol) in dry acetonitrile (15 mL) in a sealed tube was stirred for 48 h at room temperature; then, refluxed for 2 days under an argon atmosphere. The reaction mixture filtered off and the volatile materials were evaporated under vacuum. The residue was purified by silica-gel column chromatography with n-hexane/DCM (gradient 1/2, v/v) as the eluent. The desired material was obtained as a yellow solid (yield 80%). IR (ATR, room temp.): 1187 cm^{-1} (P=N); 949 cm^{-1} (P-O). ^{31}P NMR (500 MHz, $CDCI_3$) δ 9.52 (s, 3P, N_3P_3 ring); ^{1}H NMR (500 MHz, $CDCI_3$) δ 8.43 (s, 1H), 8.12 (d, J =8.8 Hz, 2H), 7.90 (d, J =8.3 Hz, 2H), 7.50 (d, J =7.7 Hz, 2H), 7.31 (d, J= 7.4 Hz, 2H), 7.24-7.18 (m, 4H) ppm; ^{13}C NMR (125 MHz, $CDCI_3$) δ 150.50, 142.50, 141.62, 135.78, 130.75, 130.72, 129.97, 128.55, 128.25, 127.20, 125.50, 125.32, 124.61, 123.96, 123.03, 122.34 ppm; MALDI TOF (m/z) calc. 2015.740, found: 2015.776 m/z.

2.3.3. Synthesis of compound 6 (octakis(4-hydroxyphenylanthracene-9-carboxylate) cyclotetraphophazene)

A mixture of 2,2,4,4,6,6,8, 8-octakis (hydroxyphenoxy) cyclotetraphosphazatetraene (**4**; 250 mg, 0.237 mmol), 9-Anthracenecarboxylic acid (527 mg, 2.37 mmol), DMAP (404 mg, 3.31 mmol) and DCC (585 mg, 2.84 mmol) in dry acetonitrile (15 mL) in a sealed tube was stirred for 48 h at room temperature; then, refluxed for 2 days under an argon atmosphere. The reaction mixture filtered off and the volatile materials were evaporated under vacuum. The residue was purified by silica-gel column chromatography with n-hexane/DCM (gradient 1/3, v/v) as the eluent. The desired material was obtained as a yellow solid (yield 79%). IR (ATR, room temp.): 1187 cm^{-1} (P=N); 949 cm^{-1} (P-O). ^{31}P NMR (500 MHz, $CDCI_3$) δ -11.29 (s, 4P, N_4P_4 ring); ^{1}H NMR (500 MHz, $CDCI_3$) δ 8.42 (s, 1H), 8.12 (d, J = 8.5 Hz, 2H), 7.87 (d, J =

8.1 Hz, 2H), 7.52 (d, J =8.8 Hz, 2H), 7.37 (d, J =8.4 Hz, 2H), 7.24-7.12 (m, 4H) ppm; ^{13}C NMR (125 MHz, $CDCl_3$) δ 151.55, 142.72, 139.93, 135.81, 130.73, 128.35, 128.28, 127.64, 127.19, 126.80, 126.07, 125.55, 125.32, 124.91, 124.70, 122.30 ppm; MALDI TOF (m/z) calc. 2687.650, found: 2687.166 m/z.

3. Results and Discussions

The compounds **1**-**4** and precursor were obtained according to literature [25-27, 30, 37]. They were characterized by standard spectroscopic techniques and X-ray crystallography. The target compounds **5** and **6** were synthesized by esterification reaction of **2** and **4** with 9-anthracene carboxylic acid, respectively (Scheme S1 and Figure 1). The esterification reactions were carried out by using DMAP and DCC as an acyl transfer reagent and dehydrating agent in acetonitrile. After filtration of reaction mixture, compound **5** and **6** were obtained by column chromatography with using n-hexane/DCM (v/v) as eluent and silica gel as stationary phase. Characterization of all synthesized compounds were performed by ^{1}H, ^{13}C and ^{31}P NMR, and mass spectrometry (MALDI-TOF) and obtained result in a good agreement with predicted structures. For instances, ^{1}H NMR of -OH of benzene moieties of compound **2** and **4** were observed at δ=8.33 and δ=8.38 ppm which were disappeared after esterification reactions as expected (Figure S2 and S6) [25, 37]. In addition, the integration of aromatic proton signals of anthracene group to the benzene group in ^{1}H NMR spectrum of compound **5** and **6** nearly 9:4 which demonstrated predicted structure as shown in Figure 1. ^{31}P NMR of compound **5** and **6** showed only singlet peaks at δ=9.52 ppm and δ=-11.29 ppm, respectively (Figure S1 and S5).

3.1. Thermal Properties

The thermal stability of the compounds **5** and **6** were followed by thermogravimetric analysis (TGA) and differential scanning calorimetry (DSC) which are given at Figure S10 and

S11. According to the TGA thermograms of compounds **5** and **6**, the compounds exhibit very high thermal stability with decomposition temperatures (T_d) in the range of 300–350 °C. The decomposition onset temperatures (T_{on}) are 310 °C for compound **5** and 300 °C for compound **6**. Also, the glass transition temperatures (T_g) of compounds are 161 °C for compound **5** and 183°C for compound **6**.

3.2. Optical and Chemosensor Properties

Optical and chemosensor behaviors of compound **5**, **6** and precursor were studied in THF with UV/vis and fluorescence spectroscopies. UV/Vis absorption and fluorescence signals of the concentration of $5x10^{-5}$ M for compounds **5**, **6** and precursor are shown in Figure 2 and Stokes shifts are given at Figure S12. The major absorption features of compounds **5** and **6** are same with their precursor. It is well known that phosphazene cores ($N_3P_3Cl_6$ or $N_4P_4Cl_8$) are optically inactive in UV/vis region, therefore they do not affect the ground state absorption properties of the attached dyes [38]. It can be seen form Figure 2b, emission of compounds **5**, **6** and precursor demonstrated broad emission bands which centered at 475 nm (λ_{ex}=365 nm). In addition to the emission band of compound **5** is slightly broader than that of compound **6** because of reflection of emission of the excimer anthracene units which are originated from intramolecular π···π interactions of the narrower cyclotriphosphazene platform. Fluorescence quantum yields (Φ_f) of the target compounds were calculated with comparative method (Eq. (1)) where 0.1 M H_2SO_4 solution of quinine sulfate as a standard [39, 40]. The concentration of each solution were fixed at $1x10^{-5}$ M. Fluorescence quantum yields (Φ_f) of compound **5** and **6** were calculated as 0.18 and 0.07, respectively.

$$\Phi_F = \Phi_F(\mathrm{Std}) \frac{F \,.\, A_{\mathrm{Std}} \,.\, n^2}{F_{\mathrm{Std}} \,.\, A \,.\, n^2_{\mathrm{Std}}} \qquad (1)$$

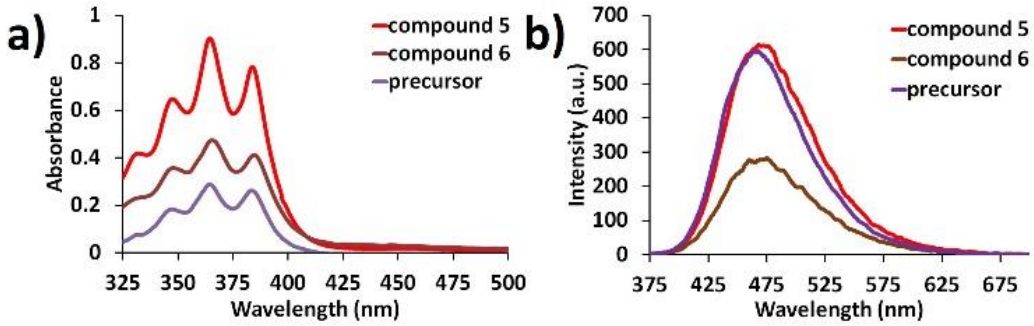

Figure 2. (a) UV/vis absorption and (b) fluorescence spectra of $5x10^{-5}$ M **5**, **6** and precursor. (THF, λ_{ex}=365 nm.)

Anthracene and its derivatives have extensively been used as fluorescence probes for explosive detection thanks to strong photoluminescence characteristics and π-electron-richness [41]. Chemosensor behaviors of compounds **5**, **6** and precursor were examined by fluorescence spectroscopy with nitrobenzene, nitrophenol, TNT, picric acid and RDX which are commonly use NACs. When compared the structure of TNT and other NACs, it can be seen that the quenching efficiency of TNT could be more effective than NACs. This observation may exist because of the three nitro-groups on its structure, which making the structure have lowest electron density [42, 43]. According to results, only TNT changed the fluorescence emission which observed at 475 nm (anthracene emission) as shown in Figure 3a and Figure 3b where other common analytes did not cause any significant changes in fluorescence emission. Also, there have not been any changes in fluorescence emissions of precursor upon addition of 500 ppm of TNT, Figure 3c. In addition, spectrofluorometric titration was performed to understand the interactions of the compounds **5** and **6** with TNT. As can be seen from Figure 4, compounds **5** (Figure 4a) and **6** (Figure 4b) with gradually increased concentration of TNT showed linear range of TNT. According to obtained data from fluorescence signals, the limit of detection (LOD) of compounds **5** and **6** for TNT were determined as 8.35 ppm ($3.67x10^{-5}$ M) and 6.43 ppm ($2.83x10^{-5}$ M), respectively, pointing a high detection sensitivity. LODs were calculated

based on 3σ/K, σ is the deviation of blank solution signal, K is slope of the calibration curve (Figure 4a and Figure 4b) [44-46]. Stoichiometry of compounds **5**, **6** with TNT were investigated with the method of continuous variation (Job's plot analyses, Figure S13). As can be seen from Job's analyses which obtained according to emission data change, 1:1 complexation was observed for compounds **5**, **6** with TNT. In addition, association constants for complexation of compounds **5**, **6** with TNT were determined as 4.39×10^4 and 4.73×10^4 M^{-1}, respectively, with using Benesi–Hildebrand equation (Figure S14) [47]. In addition, precision of **5** and **6** were evaluated for TNT detection. Therefore, ten measurements were performed for 500 ppm and 250 ppm TNT under the same experimental conditions and relative standard deviations (RSDs %) were calculated as 1.04 % and 2.05 %.

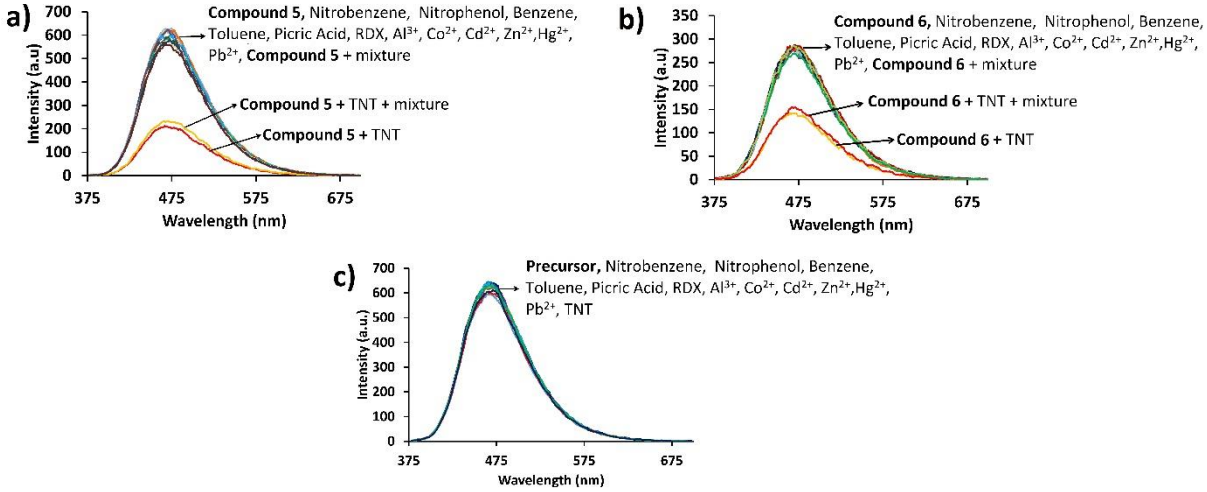

Figure 3. The selectivity of 5×10^{-5} M **5** (a), 5×10^{-5} M **6** (b) and 1×10^{-5} M precursor (c) (THF, λ_{ex}=365 nm).

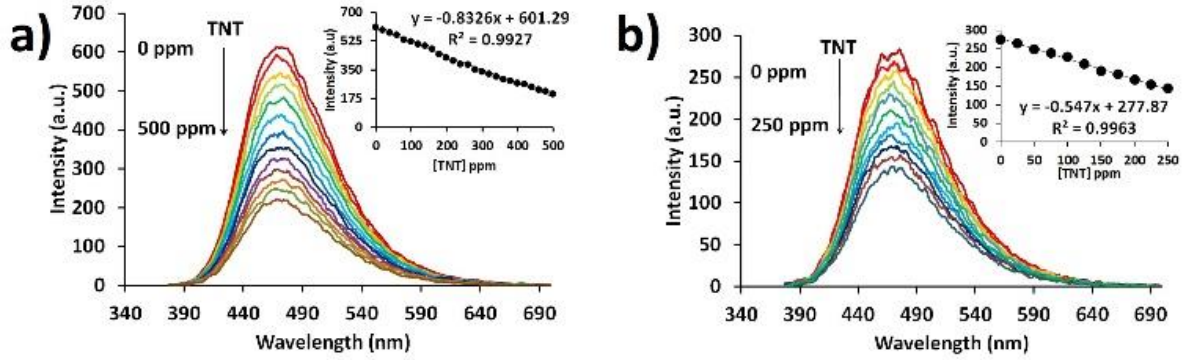

Figure 4. Spectrofluorometric titration of $5x10^{-5}$ M **5** (a), and $5x10^{-5}$ M **6** (b) with increased amount of TNT in THF solution. Excitation wavelength is 365 nm. The insets; linear range of **5** and **6** versus TNT.

3.3. Quenching Mechanism

Fluorescence quenching can occur in two different ways: static and dynamic quenching mechanism, which are completely different processes from each other. In static quenching, non-fluorescent fluorophore-quencher complex form by fluorophore and quencher in ground state. This non-fluorescent complex causes to quench of the fluorescence signal. On the other hand, in dynamic quenching process, the excited molecules of quencher and fluorophore collides and signal of the fluorophore quenches with this collision [48]. Therefore, it can be said that dynamic quenching is a diffusion-controlled process. For these reasons, fluorescence lifetime of dyes does not affect in static quenching process. However, this is completely different in the dynamic quenching process and fluorescence lifetime of fluorophore tend to decrease. In addition, concentration of quencher can give information about quenching process via fluorescence intensity changing [22]. Based on these informations, fluorescence lifetime and intensity changing of fluorophore with quencher (TNT) were measured in different concentration. To calculate those values, Stern-Volmer relationship were used [49] (2).

$$\frac{I_0}{I} = K_{SV}[Q] + 1 \qquad (2)$$

Quencher (Q) is TNT for our detection method and in this equation, fluorescence signal of compounds **5** and **6** are shown as I_0 (in absence of TNT) and I (in presence of TNT). Also, K_{SV} and Q represent the Stern-Volmer constant and concentration of TNT, respectively. According to Stern-Volmer equation, a plot of I_0/I - [TNT] gave linear graph where y-axis intercept=1 (Figure S15). Therefore, it can be said that static quenching is effective in quenching of fluorescence signal [50]. In addition, fluorescence lifetime measurements in the absence and presence of TNT for compounds **5** and **6** were performed and illustrated in Figure S15. Fluorescence lifetimes were calculated as 1.998±0.001 ns and 1.740±0.002 ns for compound **5** and compound **5** + TNT, respectively, and 1.317±0.004 ns, 1.284±0.006 ns for compound **6** and compound **6** + TNT, respectively (Figure 5 and Figure S16). It is clear the fluorescence lifetimes of compounds **5** and **6** do not change obviously by the addition of 500 ppm and 250 ppm of TNT for compounds **5** and **6**, respectively and τ_0/τ are approximately equal to 1. This result showed that quenching of fluorescence signal occurred by the static quenching in a ground-state with non-fluorescent complex formation (compound **5** + TNT and compound **6** + TNT).

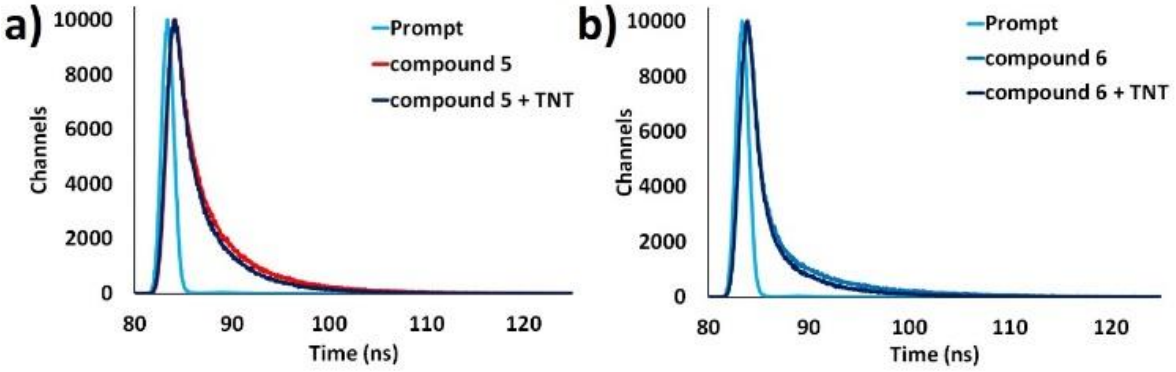

Figure 5. Fluorescence lifetime decay profiles of a) compound **5** and compound **5** + TNT, b) compound **6** and compound **6** + TNT using laser excitation source of 390 nm.

It is well-known that fluorescence detection can be achieved using the relatively the lowest unoccupied molecular orbitals (LUMO) energies of the explosive material. Because, LUMO of explosive materials can accept an excited electron from the fluorophore [51, 52]. In other words, when NACs interact with a fluorophore, the excited electron in the fluorophore can be transferred to the LUMO of the NACs instead of relaxing back to the ground state, resulting the emission changes. We assumed that there is a close relationship between the LUMO energy levels of compound **5**, **6** and TNT, causing fluorescence emission to remarkably be quenched by only TNT, even in the presence of other competing analogues, such as nitrobenzene, nitrophenol, picric acid, toluene or benzene. To confirm this assumption, HOMO and LUMO energy levels of compounds **5** and **6** were measured by the cyclic voltammetry. The cyclic voltammetry studies of compounds **5** and **6** (given in the SI as Figure S17) showed that the lowest unoccupied molecular orbital energy (LUMO) is -3.51 eV for compound **5** and -3.67 eV for compound **6**. Their LUMO energies differ only 0.16 eV. Thus, it seems there is a relationship between sensitivity and LUMO energy level of the analytes. Secondly, since TNT has a lower LUMO orbital energy, -3.7 eV [42], it can accept an electron from excited state of those compounds. LUMO of fluorophores (compound **5** and **6**) and TNT LUMO band gap were much closed to each other as expected because of phosphazene compounds known as optically inert in UV/vis radiation as mentioned.

3.4. Theoretical Calculations

Even absorption (Figure 2a) and fluorescence spectra (Figure 2b) of compounds **5** and **6** were very similar to their precursor, their sensor properties are fully different (Figure 3). This situation can be explained by that the anthracene groups are projected above and below the cyclophosphazene plane, producing the non-covalent π···π interaction between anthracene and TNT. Hence, we carried out quantum chemical calculations to obtain equilibrium structures of

compounds **5** and **6** with TNT and to estimate their HOMO-LUMO energies. All calculations were completed in the gas phase with standard density functional theory (DFT) the level of B3LYP using 6-31G (d,p) and performed with the Gaussian09 [53] package. The optimized geometries of compounds **5** and **6** with TNT, **5**-TNT and **6**-TNT, respectively, are shown in Figure 6. The optimized structures showed that the space between the anthracene and TNT molecule in the **6**–TNT complex structure is smaller and more planer than that of the **5**–TNT. This conformational change for donor-acceptor systems may reflect disparities in the charge-transfer quenching properties [54]. As one can see from the frontier orbitals given in Figure 7, the highest occupied molecular orbitals (HOMO) are located on the anthracene for both complex structures.

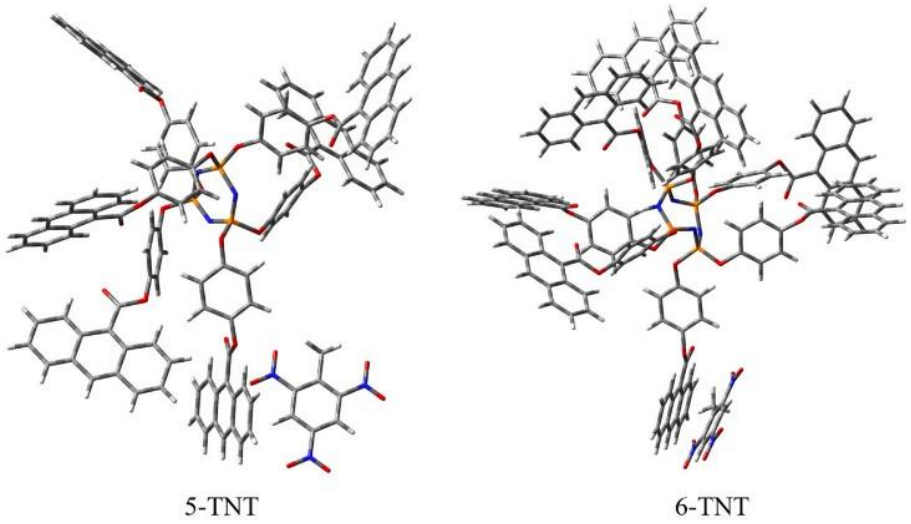

Figure 6. Optimized geometries of compound **5** and **6** with TNT.

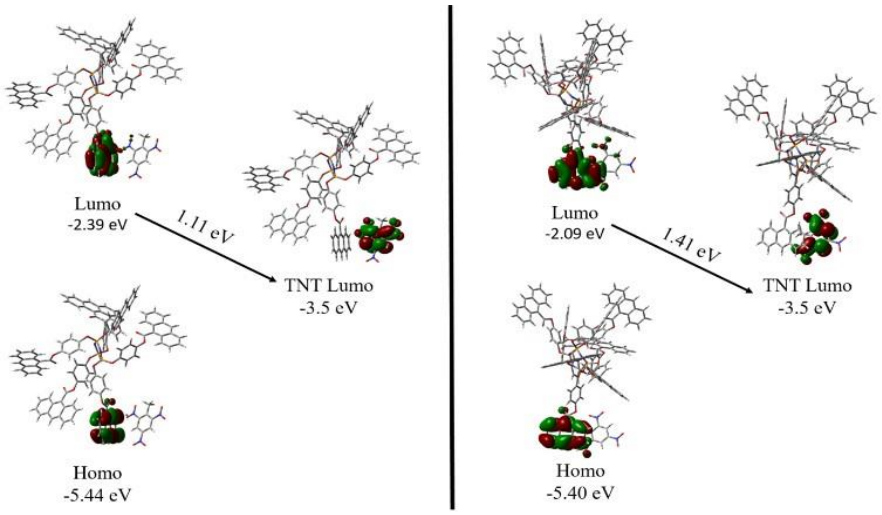

Figure 7. Frontier orbitals of **5**-TNT (left) and **6**-TNT (right) with B3LYP level of theory.

Although, their provided HOMO energies are almost similar (-5.44 eV for **5**-TNT and -5.40 eV for **6**-TNT), LUMO are different (-2.39 eV for **5**-TNT and -2.09 eV for **6**-TNT) from each other. This result indicates that there is an intermolecular π···π interaction between the anthracene and TNT molecule on the complex structures, which is influenced by position of the TNT molecule. Moreover, the order of the orbitals on the complex structures predicted by DFT confirms the experimental findings that the LUMO orbital for TNT is lower than anthracene. Thus, there is an energy transfer from LUMO of anthracene to LUMO of TNT. The energy gap between these two orbitals are 1.11 eV for **5**-TNT and 1.41 eV for **6**-TNT.

Table 1: The comparison of developed chemosensors with some previously TNT reports

Sensing System	**Linear Range (M)**	**LOD (M)**	**RSD%**	**Ref.**
cross-linking electropolymerized films	$1.0x10^{-5}$-$1.0x10^{-4}$	$1.0x10^{-5}$	N.r	[55]
PPV functionalized mesoporous silica nanoparticles with graphene oxide	0-$2.4x10^{-6}$	$1.3x10^{-7}$	N.r	[56]
pyrimidine derivatives	$1.26x10^{-1}$-$5.61x10^{-4}$	$2.77x10^{-3}$	N.r	[57]
CdSe quantum dots	$1.0x10^{-7}$–$5.0x10^{-5}$	$2.0x10^{-8}$	3.4	[58]
MIPs@CDs	$5.0x10^{-7}$-$2.0x10^{-5}$	$1.7x10^{-8}$	3.4-5.0	[59]
conjugated polymer nanoparticles	N.r	$1.0×10^{-5}$ $7.0x10^{-5}$	N.r	[60]
5	$2.2x10^{-6}$-$2.2x10^{-3}$	$3.67x10^{-5}$	1.04	PW
6	$8.8x10^{-7}$-$1.1x10^{-3}$	$2.83x10^{-5}$	2.05	PW

*N.r: not reported; PW: present work

4. Conclusion

Newly synthesized fluorescent anthracene-decorated dendrimeric cyclophosphazenes by esterification reaction compounds are highly soluble in common organic solvents, have high thermal stability and high glass transition temperatures (T_g). Considering the spectroscopic findings described above, those compounds exhibit high binding affinity and selectivity towards TNT, but not for other NACs such as nitrobenzene, nitrophenol, picric acid, toluene or benzene. The predicted computational results support experimental findings that there is a close relationship between anthracene and TNT molecule in the complex. Moreover, our novel system has moderate LOD, low RSD %, high selectivity, low cost, simple and time friendly compared to the reports focusing on TNT detection with similar approach in the (Table 1). According to obtained results, it is worthy of note that synthetic cyclophosphazenes based on dendrimeric materials can be designed and developed to get more efficient new fluorescence sensor systems for not only TNT but also other NACs, which are known as environmental pollutant and toxic to living organisms.

Acknowledgment

The research was supported by the TÜBİTAK grant 214Z259. The numerical calculations reported in this paper were fully performed at TUBITAK ULAKBIM, High Performance and Grid Computing Center (TRUBA resources).

References

[1] Y. Salinas, R. Martínez-Máñez, M.D. Marcos, F. Sancenón, A.M. Costero, M. Parra, S. Gil, Optical chemosensors and reagents to detect explosives, Chemical Society Reviews, 41 (2012) 1261-1296.

[2] S.-W. Zhang, T.M. Swager, Fluorescent Detection of Chemical Warfare Agents: Functional Group Specific Ratiometric Chemosensors, Journal of the American Chemical Society, 125 (2003) 3420-3421.

[3] X. Liu, Y. Ji, Y. Zhang, H. Zhang, M. Liu, Oxidized multiwalled carbon nanotubes as a novel solid-phase microextraction fiber for determination of phenols in aqueous samples, Journal of Chromatography A, 1165 (2007) 10-17.

[4] K. Zhang, H. Zhou, Q. Mei, S. Wang, G. Guan, R. Liu, J. Zhang, Z. Zhang, Instant Visual Detection of Trinitrotoluene Particulates on Various Surfaces by Ratiometric Fluorescence of Dual-Emission Quantum Dots Hybrid, Journal of the American Chemical Society, 133 (2011) 8424-8427.

[5] S. Chen, Q. Zhang, J. Zhang, J. Gu, L. Zhang, Synthesis of two conjugated polymers as TNT chemosensor materials, Sensors and Actuators B: Chemical, 149 (2010) 155-160.

[6] C. Nistor, A. Oubiña, M.-P. Marco, D. Barceló, J. Emnéus, Competitive flow immunoassay with fluorescence detection for determination of 4-nitrophenol, Analytica Chimica Acta, 426 (2001) 185-195.

[7] J.A. Padilla-Sánchez, P. Plaza-Bolaños, R. Romero-González, A. Garrido-Frenich, J.L. Martínez Vidal, Application of a quick, easy, cheap, effective, rugged and safe-based method for the simultaneous extraction of chlorophenols, alkylphenols, nitrophenols and cresols in agricultural soils, analyzed by using gas chromatography–triple quadrupole-mass spectrometry/mass spectrometry, Journal of Chromatography A, 1217 (2010) 5724-5731.

[8] D. Hofmann, F. Hartmann, H. Herrmann, Analysis of nitrophenols in cloud water with a miniaturized light-phase rotary perforator and HPLC-MS, Anal Bioanal Chem, 391 (2008) 161-169.

[9] S. Rochat, T.M. Swager, Conjugated Amplifying Polymers for Optical Sensing Applications, ACS Applied Materials & Interfaces, 5 (2013) 4488-4502.

[10] T.L. Andrew, T.M. Swager, A Fluorescence Turn-On Mechanism to Detect High Explosives RDX and PETN, Journal of the American Chemical Society, 129 (2007) 7254-7255.

[11] Z. Hu, B.J. Deibert, J. Li, Luminescent metal–organic frameworks for chemical sensing and explosive detection, Chemical Society Reviews, 43 (2014) 5815-5840.

[12] S.S. Nagarkar, A.V. Desai, P. Samanta, S.K. Ghosh, Aqueous phase selective detection of 2,4,6-trinitrophenol using a fluorescent metal–organic framework with a pendant recognition site, Dalton Transactions, 44 (2015) 15175-15180.

[13] G. Das, B.P. Biswal, S. Kandambeth, V. Venkatesh, G. Kaur, M. Addicoat, T. Heine, S. Verma, R. Banerjee, Chemical sensing in two dimensional porous covalent organic nanosheets, Chemical Science, 6 (2015) 3931-3939.

[14] P.E. Shaw, S.S.Y. Chen, X. Wang, P.L. Burn, P. Meredith, High-Generation Dendrimers with Excimer-like Photoluminescence for the Detection of Explosives, The Journal of Physical Chemistry C, 117 (2013) 5328-5337.

[15] G. Tang, S.S.Y. Chen, P.E. Shaw, K. Hegedus, X. Wang, P.L. Burn, P. Meredith, Fluorescent carbazole dendrimers for the detection of explosives, Polymer Chemistry, 2 (2011) 2360-2368.

[16] G.H. Shi, Z.B. Shang, Y. Wang, W.J. Jin, T.C. Zhang, Fluorescence quenching of CdSe quantum dots by nitroaromatic explosives and their relative compounds, Spectrochimica Acta Part A: Molecular and Biomolecular Spectroscopy, 70 (2008) 247-252.

[17] G.V. Zyryanov, D.S. Kopchuk, I.S. Kovalev, E.V. Nosova, V.L. Rusinov, O.N. Chupakhin, Chemosensors for detection of nitroaromatic compounds (explosives), Russian Chemical Reviews, 83 (2014) 783-819.

[18] N. Dey, S.K. Samanta, S. Bhattacharya, Selective and Efficient Detection of Nitro-Aromatic Explosives in Multiple Media including Water, Micelles, Organogel, and Solid Support, ACS Applied Materials & Interfaces, 5 (2013) 8394-8400.

[19] T. Caron, E. Pasquinet, A. van der Lee, R.B. Pansu, V. Rouessac, S. Clavaguera, M. Bouhadid, F. Serein-Spirau, J.-P. Lère-Porte, P. Montméat, Efficient Sensing of Explosives by Using Fluorescent Nonporous Films of Oligophenyleneethynylene Derivatives Thanks to Optimal Structure Orientation and Exciton Migration, Chemistry – A European Journal, 20 (2014) 15069-15076.

[20] E. Özcan, S.O. Tümay, H.A. Alidağı, B. Çoşut, S. Yeşilot, A new cyclotriphosphazene appended phenanthroline derivative as a highly selective and sensitive OFF–ON fluorescent chemosensor for Al3+ ions, Dyes and Pigments, 132 (2016) 230-236.

[21] S.O. Tümay, A. Uslu, H. Ardıç Alidağı, H.H. Kazan, C. Bayraktar, T. Yolaçan, M. Durmuş, S. Yeşilot, A systematic series of fluorescence chemosensors with multiple binding sites for Hg(ii) based on pyrenyl-functionalized cyclotriphosphazenes and their application in live cell imaging, New Journal of Chemistry, 42 (2018) 14219-14228.

[22] S.O. Tümay, S.Y. Sarıkaya, S. Yeşilot, Novel iron(III) selective fluorescent probe based on synergistic effect of pyrene-triazole units on a cyclotriphosphazene scaffold and its utility in real samples, Journal of Luminescence, 196 (2018) 126-135.

[23] B. Çoşut, S. Yeşilot, Synthesis, thermal and photophysical properties of naphthoxycyclotriphosphazenyl-substituted dendrimeric cyclic phosphazenes, Polyhedron, 35 (2012) 101-107.

[24] H.J. Bolink, S.G. Santamaria, S. Sudhakar, C. Zhen, A. Sellinger, Solution processable phosphorescent dendrimers based on cyclic phosphazenes for use in organic light emitting diodes (OLEDs), Chemical Communications, (2008) 618-620.

[25] B. Çoşut, S. Yeşilot, M. Durmuş, A. Kılıç, Synthesis and fluorescence properties of hexameric and octameric subphthalocyanines based cyclic phosphazenes, Dyes and Pigments, 98 (2013) 442-449.

[26] G. Egemen, M. Hayvalı, Z. Kılıç, A.O. Solak, Z. Üstündağ, Phosphorus-nitrogen compounds Part 17: The synthesis, spectral and electrochemical investigations of porphyrino-phosphazenes, Journal of Porphyrins and Phthalocyanines, 14 (2010) 227-234.

[27] A. Okumuş, S. Bilge, Z. Kılıç, A. Öztürk, T. Hökelek, F. Yılmaz, Phosphorus–nitrogen compounds. Part 20: Fully substituted spiro-cyclotriphosphazenic lariat (PNP-pivot) ether derivatives, Spectrochimica Acta Part A: Molecular and Biomolecular Spectroscopy, 76 (2010) 401-409.

[28] H.A. Alidağı, F. Hacıvelioğlu, S.O. Tümay, B. Çoşut, S. Yeşilot, Synthesis and spectral properties of fluorene substituted cyclic and polymeric phosphazenes, Inorganica Chimica Acta, 457 (2017) 95-102.

[29] H.A. Alidağı, S.O. Tümay, A. Şenocak, S. Yeşilot, Pyrene functionalized cyclotriphosphazene-based dyes: Synthesis, intramolecular excimer formation, and fluorescence receptor for the detection of nitro-aromatic compounds, Dyes and Pigments, 153 (2018) 172-181.

[30] T.B. Petersen, R. Khan, B. Olofsson, Metal-Free Synthesis of Aryl Esters from Carboxylic Acids and Diaryliodonium Salts, Organic Letters, 13 (2011) 3462-3465.

[31] Bruker(2014), APEX2, version 2014.11-0, Bruker AXS Inc., Madison, Wisconsin, USA.

[32] Bruker(2013), SAINT, version V8.34A, Bruker AXS Inc., Madison, Wisconsin, USA.

[33] Bruker(2014), SADABS, version 2014/4, Bruker AXS Inc., Madison, Wisconsin, USA.

[34] Bruker(2010), SHELXTL, version 6.14, Bruker AXS Inc., Madison, Wisconsin, USA.

[35] A. Spek, Structure validation in chemical crystallography, Acta Crystallographica Section D, 65 (2009) 148-155.

[36] C.F. Macrae, P.R. Edgington, P. McCabe, E. Pidcock, G.P. Shields, R. Taylor, M. Towler, J. van de Streek, Mercury: visualization and analysis of crystal structures, Journal of Applied Crystallography, 39 (2006) 453-457.

[37] J. Barberá, M. Bardají, J. Jiménez, A. Laguna, M.P. Martínez, L. Oriol, J.L. Serrano, I. Zaragozano, Columnar Mesomorphic Organizations in Cyclotriphosphazenes, Journal of the American Chemical Society, 127 (2005) 8994-9002.

[38] S. Çetindere, S.O. Tümay, A. Kılıç, M. Durmuş, S. Yeşilot, Synthesis and physico-chemical properties of cyclotriphosphazene-BODIPY conjugates, Dyes and Pigments, 139 (2017) 517-523.

[39] W.H. Melhuish, QUANTUM EFFICIENCIES OF FLUORESCENCE OF ORGANIC SUBSTANCES: EFFECT OF SOLVENT AND CONCENTRATION OF THE FLUORESCENT SOLUTE1, The Journal of Physical Chemistry, 65 (1961) 229-235.

[40] S. Fery-Forgues, D. Lavabre, Are Fluorescence Quantum Yields So Tricky to Measure? A Demonstration Using Familiar Stationery Products, Journal of Chemical Education, 76 (1999) 1260.

[41] H. Sohn, M.J. Sailor, D. Magde, W.C. Trogler, Detection of Nitroaromatic Explosives Based on Photoluminescent Polymers Containing Metalloles, Journal of the American Chemical Society, 125 (2003) 3821-3830.

[42] A. Saxena, M. Fujiki, R. Rai, G. Kwak, Fluoroalkylated Polysilane Film as a Chemosensor for Explosive Nitroaromatic Compounds, Chemistry of Materials, 17 (2005) 2181-2185.

[43] S.J. Toal, W.C. Trogler, Polymer sensors for nitroaromatic explosives detection, Journal of Materials Chemistry, 16 (2006) 2871-2883.

[44] C.A. Parker, W.T. Rees, Correction of fluorescence spectra and measurement of fluorescence quantum efficiency, Analyst, 85 (1960) 587-600.

[45] Y. Gabe, Y. Urano, K. Kikuchi, H. Kojima, T. Nagano, Highly Sensitive Fluorescence Probes for Nitric Oxide Based on Boron Dipyrromethene ChromophoreRational Design of Potentially Useful Bioimaging Fluorescence Probe, Journal of the American Chemical Society, 126 (2004) 3357-3367.

[46] J. Liu, Y. Lu, Rational Design of "Turn-On" Allosteric DNAzyme Catalytic Beacons for Aqueous Mercury Ions with Ultrahigh Sensitivity and Selectivity, Angewandte Chemie, 119 (2007) 7731-7734.

[47] H.A. Benesi, J.H. Hildebrand, A Spectrophotometric Investigation of the Interaction of Iodine with Aromatic Hydrocarbons, Journal of the American Chemical Society, 71 (1949) 2703-2707.

[48] J.R. Lakowicz, Plasmonics in Biology and Plasmon-Controlled Fluorescence, Plasmonics (Norwell, Mass.), 1 (2006) 5-33.

[49] K.W. Cha, K.W. Park, Determination of iron(III) with salicylic acid by the fluorescence quenching method, Talanta, 46 (1998) 1567-1571.

[50] P.K. Behera, T. Mukherjee, A.K. Mishra, Simultaneous presence of static and dynamic component in the fluorescence quenching for substituted naphthalene—CCl4 system, Journal of Luminescence, 65 (1995) 131-136.

[51] J.C. Sanchez, A.G. DiPasquale, A.L. Rheingold, W.C. Trogler, Synthesis, Luminescence Properties, and Explosives Sensing with 1,1-Tetraphenylsilole- and 1,1-Silafluorene-vinylene Polymers, Chemistry of Materials, 19 (2007) 6459-6470.

[52] A.F. Khasanov, D.S. Kopchuk, I.S. Kovalev, O.S. Taniya, K. Giri, P.A. Slepukhin, S. Santra, M. Rahman, A. Majee, V.N. Charushin, O.N. Chupakhin, Extended cavity pyrene-based iptycenes for the turn-off fluorescence detection of RDX and common nitroaromatic explosives, New Journal of Chemistry, 41 (2017) 2309-2320.

[53] M.J. Frisch, G.W. Trucks, H.B. Schlegel, G.E. Scuseria, M.A. Robb, J.R. Cheeseman, et al., Gaussian 09, Gaussian, Inc., Wallingford CT, 2009.

[54] Y.H. Lee, H. Liu, J.Y. Lee, S.H. Kim, S.K. Kim, J.L. Sessler, Y. Kim, J.S. Kim, Dipyrenylcalix[4]arene—A Fluorescence-Based Chemosensor for Trinitroaromatic Explosives, Chemistry – A European Journal, 16 (2010) 5895-5901.

[55] H. Nie, Y. Lv, L. Yao, Y. Pan, Y. Zhao, P. Li, G. Sun, Y. Ma, M. Zhang, Fluorescence detection of trace TNT by novel cross-linking electropolymerized films both in vapor and aqueous medium, Journal of Hazardous Materials, 264 (2014) 474-480.

[56] H. Zhang, L. Feng, B. Liu, C. Tong, C. Lü, Conjugation of PPV functionalized mesoporous silica nanoparticles with graphene oxide for facile and sensitive fluorescence detection of TNT in water through FRET, Dyes and Pigments, 101 (2014) 122-129.

[57] E.V. Verbitskiy, E.B. Gorbunov, A.A. Baranova, K.I. Lugovik, K.O. Khokhlov, E.M. Cheprakova, G.A. Kim, G.L. Rusinov, O.N. Chupakhin, V.N. Charushin, New 2H-[1,2,3]triazolo[4,5-e][1,2,4]triazolo[1,5-a]pyrimidine derivatives as luminescent fluorophores for detection of nitroaromatic explosives, Tetrahedron, 72 (2016) 4954-4961.

[58] K.-Y. Yi, Application of CdSe quantum dots for the direct detection of TNT, Forensic Science International, 259 (2016) 101-105.

[59] S. Xu, H. Lu, Mesoporous structured MIPs@CDs fluorescence sensor for highly sensitive detection of TNT, Biosensors and Bioelectronics, 85 (2016) 950-956.

[60] X. Wu, H. Li, B. Xu, H. Tong, L. Wang, Solution-dispersed porous hyperbranched conjugated polymer nanoparticles for fluorescent sensing of TNT with enhanced sensitivity, Polymer Chemistry, 5 (2014) 4521-4525.

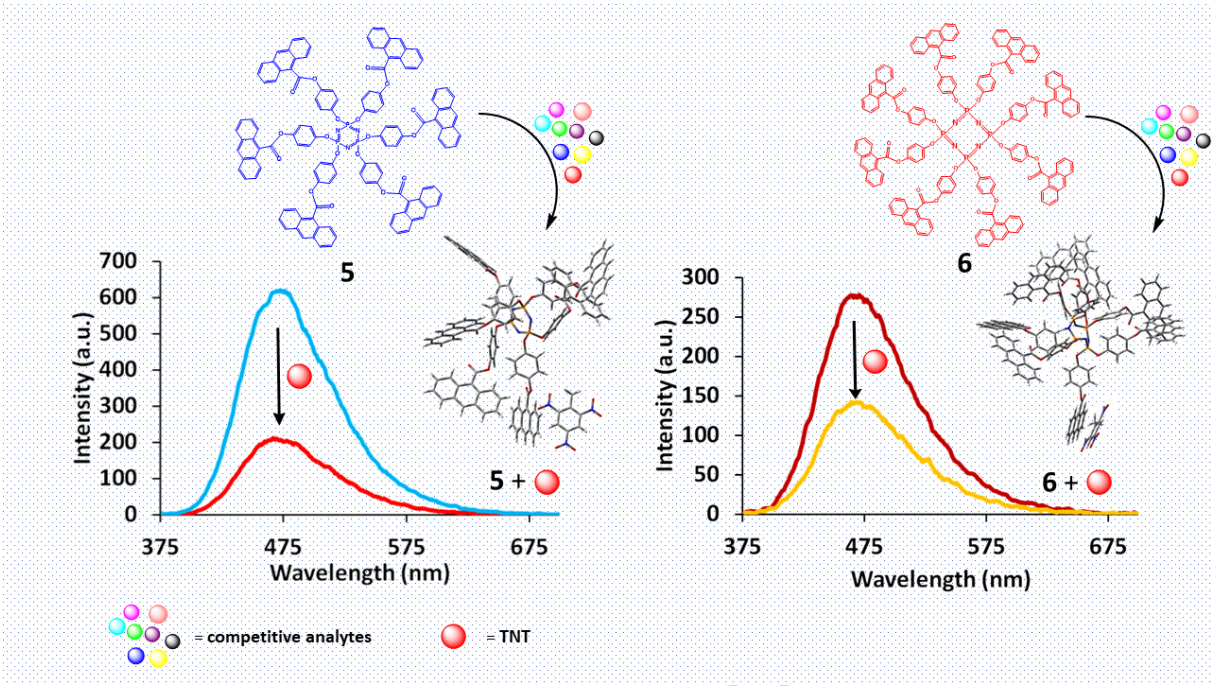

Graphical abstract

Highlights

► A new type of fluorescent chemosensors based on anthracene-decorated cyclotri- and cyclotetraphosphazenes have been synthesized.► The photophysical properties of the compounds have been studied in THF ► The Fluorescence Sensing properties of the compounds have been studied in THF ►Very selective and sensitive fluorescence sensors for detection of TNT have been obtained.